

# Synthesis and Application of Modular Phosphine–Phosphoramidite Ligands in Asymmetric Hydroformylation: Structure–Selectivity Relationship

Xiaowei Zhang,<sup>[a, b]</sup> Bonan Cao,<sup>[a]</sup> Yongjun Yan,<sup>[b]</sup> Shichao Yu,<sup>[a]</sup> Baoming Ji,<sup>[b]</sup> and Xumu Zhang\*<sup>[a]</sup>

**Abstract:** A series of hybrid phosphine–phosphoramidite ligands has been designed and synthesized in moderate yields from chiral BINOL (1,1'-bi-2-naphthol) or NOBIN (2-amino-2'-hydroxy-1,1'-binaphthyl). They have achieved highly regio- and enantioselectivities in Rh-catalyzed asymmetric hydroformylations of styrene derivatives (branched/linear ratio up to 56.6,

*ee* up to 99%), vinyl acetate derivatives (up to 98% *ee*), and allyl cyanide (up to 96% *ee*). Systematic variation of ligand structure showed that the steric

factor on the phosphoramidite moiety determined the performance of the ligand. With the increased hindrance, the branched/linear ratio rose, while the *ee* value dropped in the hydroformylation of styrene. However, the N-substituents did not influence the selectivities much.

**Keywords:** asymmetric catalysis · enantioselectivity · hydroformylation · phosphine–phosphoramidite ligands · rhodium

## Introduction

Hydroformylation is one of the most important reactions still widely used in industry that provides aldehydes directly from alkenes and syngas (CO/H<sub>2</sub>) in one single step. Millions of tons of oxo products produced worldwide per year lead to it being regarded as the largest industrially homogeneous catalytic process.<sup>[1]</sup> In particular, asymmetric hydroformylation (AHF) has attracted much attention as an atom-economic method to convert olefins into enantiomerically pure aldehydes, which can be used as important precursors for synthesizing a variety of biologically active products and fine chemicals.<sup>[1–3]</sup> Although AHF offers promising application, it is still seldom utilized by industry mainly because of several well-known challenging issues. First, highly

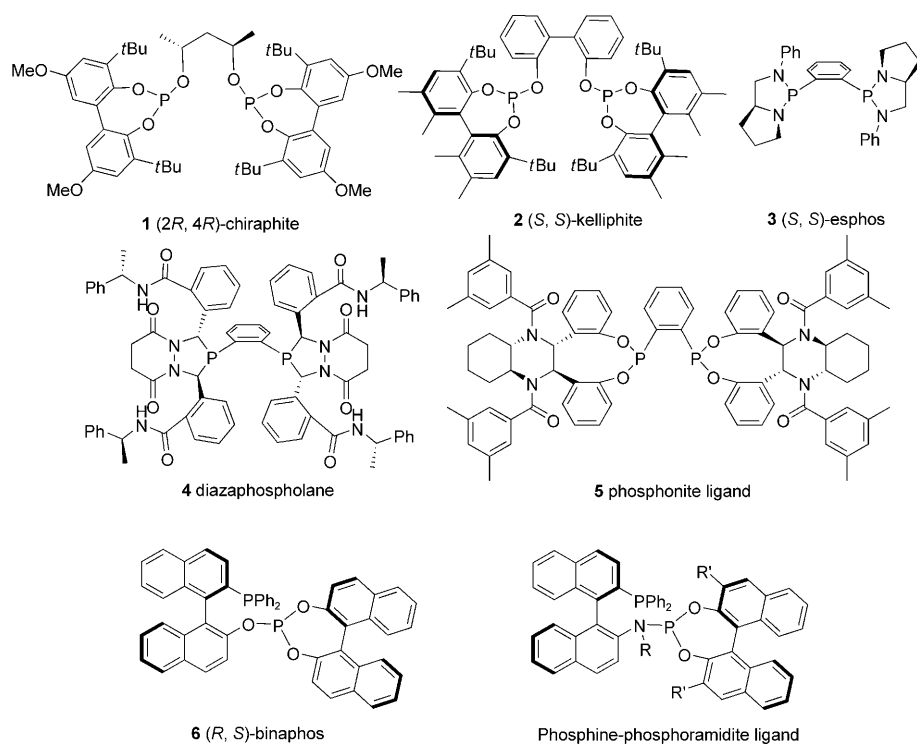
enantioselective hydroformylations are usually carried out at low temperature with relatively low reaction rate and conversion. Second, it is difficult to achieve good reactivity, regio-, and enantioselectivities under the same conditions. Finally, racemization of the aldehyde products, particularly those from styrene derivatives, is observed under hydroformylation reaction conditions.<sup>[1b]</sup>

Although new ligands that are able to provide chiral aldehydes at reasonably high temperatures without sacrificing their selectivities are highly desirable, only a few successful examples were documented in the past two decades (Scheme 1). Bidentate phosphite ligands proved to be active in AHF reactions, such as (2*R*, 4*R*)-chiraphite (**1**)<sup>[4]</sup> and (*S*, *S*)-kelliphite (**2**).<sup>[5]</sup> The former ligand shows high enantioselectivity (nearly 90% *ee*) for the hydroformylation of styrene and the latter one is effective for allyl cyanide [75% *ee*, b/l (branched/linear ratio)=16] and vinyl acetate (88% *ee*, b/l=56) at low temperature. Another class of successful ligands is the C<sub>2</sub>-symmetric bis-phospholane; for example, (*S*, *S*)-esphos (**3**),<sup>[6]</sup> reported by Wills and co-workers, provides a high selectivity for vinyl acetate (90% *ee*, b/l=16), but nearly no enantioselectivity for styrene. Landis, Klosin, and co-workers reported the diazaphospholane ligand **4** and its analogues,<sup>[7]</sup> which were applied in the AHF of styrene, vinyl acetate, and allyl cyanide with high enantioselectivities (82, 96, 87% *ee*, respectively) and regioselectivities (b/l=7, 4, 37, respectively) even at elevated temperature. Recently, a class of C<sub>2</sub>-symmetric bidentate phosphonite ligands, re-

[a] X. Zhang, B. Cao, Dr. S. Yu, Prof. Dr. X. Zhang  
Department of Chemistry and Chemical Biology and  
Department of Pharmaceutical Chemistry  
Rutgers, The State University of New Jersey  
Piscataway, New Jersey 08854 (USA)  
Fax: (+1) 732-445-6312  
E-mail: xumu@rci.rutgers.edu

[b] X. Zhang, Dr. Y. Yan, Dr. B. Ji  
Department of Chemistry  
The Pennsylvania State University  
University Park, Pennsylvania 16802 (USA)

Supporting information for this article is available on the WWW under <http://dx.doi.org/10.1002/chem.200902238>.



Scheme 1. Representative examples of chiral ligands for AHF reactions and the structure of the phosphine–phosphoramidite ligand.

ported by Ding's group, also displayed high selectivity in Rh-catalyzed AHF of the above olefins.<sup>[8]</sup> Among all the ligands reported hitherto, hybrid ligands bearing a different phosphorus structure have been regarded as the best in AHF. The major breakthrough in this area was made in 1993, when Takaya, Nozaki and co-workers reported (*R,S*)-binaphos (**6**),<sup>[9]</sup> which offered generally high enantioselectivities in the AHF of a variety of prochiral olefins (up to 94% *ee*, *b/l*=7.3 for styrene). However, with binaphos as the ligand, chiral aldehyde products can undergo racemization under certain conditions.<sup>[9b]</sup> It is still highly desirable to develop new ligands for highly enantioselective hydroformylation without racemization. Herein, we report the synthesis of a new family of hybrid phosphine–phosphoramidite ligands (as shown in Scheme 1) as well as their applications in the Rh-catalyzed AHF of styrene, vinyl acetate, allyl cyanide, and their derivatives with good to excellent regio- and enantioselectivities (up to 99% *ee*). The modular character allows systematic variation on the ligand structure, which was utilized to investigate the relationship between the ligand structure and their control of enantioselectivity. We envision that understanding of the structure–selectivity relationship can provide useful guidance for ligand design and help for optimizing the current theoretical models for AHF.

## Results and Discussion

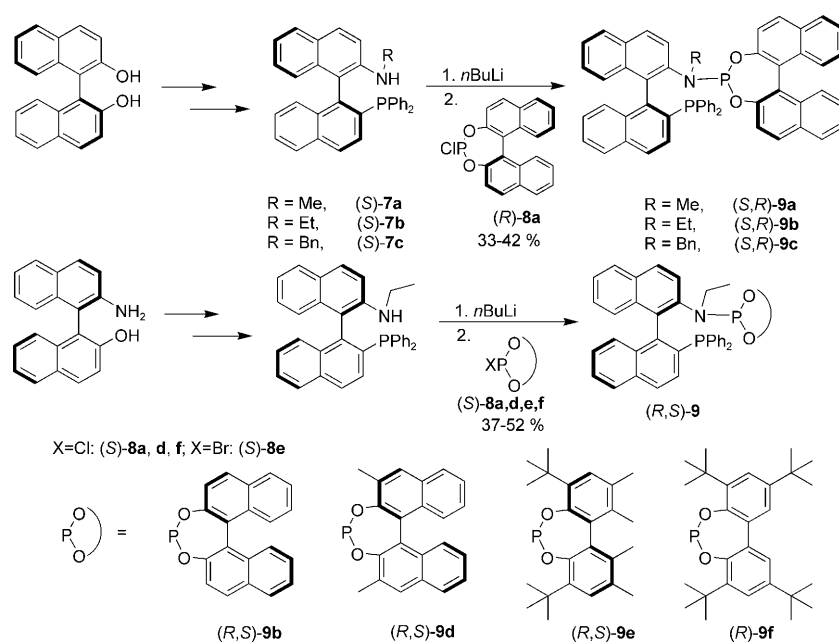
Compared to binaphos, the phosphine–phosphoramidite ligand is more electron-donating since the electronegativity

of nitrogen (3.04) is less than that of oxygen (3.44). Sterically, the N-substituent on the phosphoramidite group can make the active catalytic complex show a deeper and more closed chiral pocket than that of binaphos, based on the models from CAChe MM2 calculation.<sup>[11]</sup> Takaya and co-workers have concluded that the configuration matched (*R,S* and *S,R*)-binaphos showed better selectivity than the mismatched (*R,R* and *S,S*)-binaphos. As analogues of binaphos, the new hybrid phosphine–phosphoramidite ligands were synthesized with two enantiomerically opposite binaphthyl groups. First, we synthesized ligands **9a**, **9b** (named as YanPhos),<sup>[10]</sup> and **9c** with a methyl, ethyl, and benzyl group, respectively, attached to the nitrogen atom to investigate the influence of the N-substituents (Scheme 2). Afterward,

with an ethyl group as the N-substituent, the binaphthyl group of the phosphoramidite part was decorated with methyl groups at the 3,3'-position (ligand **9d**) or with the sterically more bulky *tert*-butyl-substituted biphenyl groups to determine the steric effect of the phosphoramidite moiety (ligand **9e** and **9f**, Scheme 2). Those bulky substituents spatially adjacent to the P atom were expected to make the chiral pocket more closed and further define the asymmetric environment around the catalytic center.

Ligands (*S,R*)-**9a**, (*S,R*)-**9b**, and (*S,R*)-**9c** were synthesized from commercially available (*S*)-BINOL (1,1'-bi-2-naphthol). Following the literature procedure,<sup>[12]</sup> the phosphine-amines (**7a–c**) were easily prepared by a sequence of well-established steps. Followed by deprotonation with *n*BuLi and quenching with the phosphorochloridite (**8a**, prepared from (*R*)-BINOL), the desired ligands (*S,R*)-**9a**, (*S,R*)-**9b**, and (*S,R*)-**9c** were obtained in moderate yield (33–42%). An alternative concise pathway to afford *N*-ethyl phosphine-amine (**7b**) starts from NOBIN (2-amino-2'-hydroxy-1,1'-binaphthyl) according to a known procedure.<sup>[13]</sup> As shown in Scheme 2, the following deprotonation and coupling with the corresponding phosphorochloridites afforded the desired ligands (*R,S*)-**9b**, (*R,S*)-**9d**, (*R,S*)-**9e**, and (*R*)-**9f**. It is worthwhile to note that all these ligands are air-stable solids.

Before applying these novel phosphine–phosphoramidite ligands in Rh-catalyzed asymmetric hydroformylation, the optimized reaction conditions were obtained by using (*R,S*)-**9b** as a representative ligand and styrene (**10**) as a standard substrate. The AHF reactions were carried out with



Scheme 2. Synthesis of phosphine–phosphoramidite ligands.

0.1 mol% of catalyst loading and 1:1 CO/H<sub>2</sub> gas. The catalyst was prepared in situ by mixing [Rh(acac)(CO)<sub>2</sub>] with ligand **9b**. The ligand/Rh ratio significantly influenced the hydroformylation reaction. As shown in Table 1, entries 1–4, increasing the ligand/Rh ratio from 1:1 to 4:1 improved both the regioselectivity (b/l from 3.0 to 7.3) and enantioselectivity (from 21 to 98% *ee*), but further increasing the ratio to 6:1 did not result in any further improvement. Screening the reaction solvent showed that nonpolar solvents, such as benzene and toluene, offered high enantioselectivities (Table 1,

entries 3, 5–8). Increasing the reaction temperature led to higher conversion but lower *ee* values (Table 1, entries 1, 9, and 10). As high as 99% *ee* was obtained when the reaction was run at 40 °C with 25% conversion, while the *ee* value dropped to 81% at 80 °C. The best temperature for this catalyst system is 60 °C where full conversion and 98% *ee* were achieved. The syngas pressure did not influence the enantioselectivity but impacted the reactivity dramatically (Table 1, entries 3, 11, and 12). The higher CO/H<sub>2</sub> pressure resulted in lower conversion, which is mainly because the equilibrium of CO coordination to the Rh center is shifted more towards carbonyl-bound Rh species at high pressure. A longer reaction time led to only a slight decrease in the enantioselectivity (Table 1, entries 3, 13, and 14). The racemization of the Rh/**9b**-catalyzed AHF was markedly lower than that of binaphos.<sup>[9b]</sup> All of the above hydroformylation reactions provided high chemoselectivities (no hydrogenation product was detected) and good regioselectivities, whereas the enantioselectivities strongly depended on reaction conditions. Entry 3 in Table 1 represents the optimized reaction conditions for phosphine–phosphoramidite ligands.

Using the optimized reaction conditions, we systematically investigated the structure–selectivity relationship of phosphine–phosphoramidite ligands. Three of the most commonly used standard substrates: styrene (**10**), vinyl acetate (**13**), and allyl cyanide (**16**) were utilized to examine the regio- and enantioselectivities of this series of ligands **9a** to **9f** in Rh-catalyzed AHF (Table 2). The impact of the N-substituent was examined by comparing the performance of ligands **9a**, **9b**, and **9c** (Table 2, entries 1–3). Increasing the steric bulk of the N-substituent from a methyl to a benzyl group slightly elevated the regioselectivity and decreased the enantioselectivity. An N-ethyl-substituted ligand, (S,R)-**9b**, provided hitherto the best enantioselectivities for Rh-

Table 1. Optimization of Rh-catalyzed asymmetric hydroformylation of styrene with (R,S)-**9b**.<sup>[a]</sup>

Entry	<b>9b</b> /Rh	Solvent	T [°C]	CO/H <sub>2</sub> [atm]	Time [h]	Conv. [%] <sup>[b]</sup>	b/l <sup>[b]</sup>	<i>ee</i> [%] <sup>[c]</sup>
1	1:1	PhH	60	10/10	24	99	3.0	21( <i>R</i> )
2	2:1	PhH	60	10/10	24	99	5.7	54( <i>R</i> )
3	<b>4:1</b>	<b>PhH</b>	<b>60</b>	<b>10/10</b>	<b>24</b>	<b>99</b>	<b>7.3</b>	<b>98(<i>R</i>)</b>
4	6:1	PhH	60	10/10	24	99	7.3	98( <i>R</i> )
5	<b>4:1</b>	<b>PhMe</b>	<b>60</b>	<b>10/10</b>	<b>24</b>	<b>99</b>	<b>7.2</b>	<b>98(<i>R</i>)</b>
6	4:1	CH <sub>2</sub> Cl <sub>2</sub>	60	10/10	24	93	10.1	97( <i>R</i> )
7	4:1	THF	60	10/10	24	95	7.3	78( <i>R</i> )
8	4:1	EtOAc	60	10/10	24	98	8.1	84( <i>R</i> )
9	4:1	PhH	40	10/10	24	25	10.1	99( <i>R</i> )
10	4:1	PhH	80	10/10	24	99	5.7	81( <i>R</i> )
11	4:1	PhH	60	20/20	24	91	8.0	98( <i>R</i> )
12	4:1	PhH	60	30/30	24	83	7.3	98( <i>R</i> )
13	4:1	PhH	60	10/10	12	87	8.1	99( <i>R</i> )
14	4:1	PhH	60	10/10	36	99	7.3	97( <i>R</i> )

[a] All reactions were carried out with substrate/Rh=1000. [b] Conversions and branched/linear ratio (b/l) were determined on the basis of <sup>1</sup>H NMR spectroscopy. [c] Determined by converting the aldehyde to the corresponding alcohol with NaBH<sub>4</sub> followed by GC analysis (Supelco's Beta Dex 225). The absolute configuration (*R*) was assigned by comparing the sign of the optical rotation of the resulting alcohol with (*R*)-2-phenylpropan-1-ol. The entries in boldface highlight key results.

Table 2. Rh-catalyzed AHF of styrene, vinyl acetate, and allyl cyanide with phosphine–phosphoramidite ligands.<sup>[a]</sup>

**10:** R = Ph  
**13:** R = AcO  
**16:** R = CNCH<sub>2</sub>

**11:** R = Ph  
**14:** R = AcO  
**17:** R = CNCH<sub>2</sub>

**12:** R = Ph  
**15:** R = AcO  
**18:** R = CNCH<sub>2</sub>

Entry	Ligand	<b>10</b>			<b>13</b>			<b>16</b>		
		Conv. [%] <sup>[b]</sup>	b/l <sup>[b]</sup>	ee [%] <sup>[b]</sup>	Conv. [%] <sup>[b]</sup>	b/l <sup>[b]</sup>	ee [%] <sup>[b]</sup>	Conv. [%] <sup>[b]</sup>	b/l <sup>[b]</sup>	ee [%] <sup>[c]</sup>
1	( <i>S,R</i> )- <b>9a</b>	99(24) <sup>[d]</sup>	6.6	97( <i>S</i> )	76	12.1	95( <i>R</i> )	97	3.8	96( <i>S</i> )
2	( <i>S,R</i> )- <b>9b</b>	<b>99(22)</b> <sup>[d]</sup>	<b>7.2</b>	<b>98(<i>S</i>)</b>	<b>76</b>	<b>14.0</b>	<b>96(<i>R</i>)</b>	<b>99</b>	<b>4.0</b>	<b>96(<i>S</i>)</b>
3	( <i>S,R</i> )- <b>9c</b>	99(22) <sup>[d]</sup>	7.1	95( <i>S</i> )	77	16.5	95( <i>R</i> )	99	4.1	93( <i>S</i> )
4	( <i>R,S</i> )- <b>9b</b>	<b>99(22)</b> <sup>[d]</sup>	<b>7.2</b>	<b>98(<i>R</i>)</b>	<b>76</b>	<b>13.5</b>	<b>96(<i>S</i>)</b>	<b>99</b>	<b>4.0</b>	<b>96(<i>R</i>)</b>
5	( <i>R,S</i> )- <b>9d</b>	96(13) <sup>[d]</sup>	8.0	91( <i>R</i> )	69	65.2	84( <i>S</i> )	89	3.0	90( <i>R</i> )
6	( <i>R,S</i> )- <b>9e</b>	99(27) <sup>[d]</sup>	27.6	66( <i>R</i> )	88	22.9	65( <i>S</i> )	95	2.5	65( <i>R</i> )
7	( <i>R</i> )- <b>9f</b>	99(29) <sup>[d]</sup>	56.6	75( <i>R</i> )	95	7.5	66( <i>S</i> )	98	2.9	69( <i>R</i> )

[a] All reactions were carried out at 60 °C in toluene with L:Rh = 4:1, substrate/Rh = 1000, 20 bar 1:1 CO/H<sub>2</sub>, and a reaction time of 24 h for styrene, vinyl acetate and a reaction time of 18 h for allyl cyanide. The entries in boldface highlight key results. [b] Conversions, branched/linear ratio and *ee* values were determined by GC analysis (Supelco's Beta Dex 225). The absolute configuration for the products **11**, **14**, and **17** were assigned by comparing the sign of the optical rotations with those in the literature.<sup>[14]</sup> [c] Determined by converting the aldehyde to the corresponding acid and then reacting with aniline to afford corresponding amide followed by HPLC analysis. [d] The number in parentheses represents the conversion of a reaction carried out for 3 h.

catalyzed AHF with 98% *ee* for styrene and 96% *ee* for vinyl acetate. Notably, with (*S,R*)-**9b** as ligand, the hydroformylation of allyl cyanide afforded as high as 96% *ee*, which is higher than the previously best enantioselectivity (94% *ee* at 49% conversion) achieved by binapine,<sup>[15]</sup> a ligand developed in our group for hydrogenation. Overall, the variation of *N*-substituent does not exert much influence on the selectivities of phosphine–phosphoramidite ligands.

As a counter enantiomer, (*R,S*)-**9b** showed regio- and enantioselectivities for all the three substrates almost equal to those achieved with (*S,R*)-**9b** as ligand, except for the opposite absolute configuration of the products (Table 2, entries 2 and 4). By fixing an *N*-ethyl group to the phosphine-amine moiety, we investigated the steric effect of the phosphite part on the regio- and enantioselectivities of phosphine–phosphoramidite ligands. (*R,S*)-**9d**, with two methyl groups at the 3,3'-position of binaphthyl part, did not display a higher enantioselectivity than the corresponding (*R,S*)-**9b** as expected (Table 2, entries 4 and 5). Unlike the case of binaphos, where the two additional methyl groups led to a much higher reactivity and enantioselectivity,<sup>[9c]</sup> (*R,S*)-**9d** resulted in decreased reactivity and *ee* values, albeit with higher regioselectivities for styrene and vinyl acetate (b/l = 8.0 and 65.2, respectively). Although possessing the even more sterically bulky phosphoramidite fragment, (*R,S*)-**9e** proved to be less effective in asymmetric induction than (*R,S*)-**9d** with only moderate *ee* values for the three substrates (66, 65, and 65%, respectively, Table 2, entry 6). The improvement was the higher regioselectivity for styrene (b/l = 27.6). To investigate the role of the chirality of the phosphoramidite unit, (*R*)-**9f** was prepared and used in AHF. In contrast to (*R,S*)-**9e**, the loss of one chiral center did not have a negative effect on the enantioselectivity, but led to slightly higher *ee* values (75, 66, and 69%, respectively, Table 2, entry 7). Notably, (*R*)-**9f** afforded a regioselectivity up to b/l = 56.6, which is the best result obtained under

these conditions to our knowledge. The overall trend is such that increasing the steric bulkiness of the phosphoramidite moiety diminishes the enantioselectivity, but benefits the regioselectivity for the AHF of styrene.

To investigate the effect of ligand structure on the catalytic activities, we applied ligands **9a–f** in the AHF of styrene with a reaction time of 3 h (as shown in parentheses in Table 2). It was found that the *N*-substituents did not influence the ligand activity very much. The conversions of styrene with ligands **9a–c** were 24, 22, and 22%, respectively. The activity of **9d** was much slower than that of the other ligands, which is possibly due to its poor solubility in toluene. Ligands **9e** and **9f** resulted in higher activity with 27% and 29% conversion, respectively.

To explain our above observation, we took advantage of the models from CAChe MM2 calculations with ligand **9b** as a reference. Based on the mechanistic studies by Takaya and co-workers, it is believed that the active catalyst [RhH(CO){(*R,S*)-**9b**}] coordinates with olefin to form a trigonal-bipyramidal complex, in which the phosphine occupies an equatorial position and the phosphate is located at an axial position that is *trans* to the hydrido ligand.<sup>[9b]</sup> Herrmann and co-workers proposed a semiquantitative theoretical model that can successfully elucidate the origin of stereodifferentiation in Rh-binaphos-catalyzed AHF.<sup>[1d,16]</sup> Because of the structural and electronegative similarity to binaphos (as shown in Scheme 1), ligand **9b** is proposed to proceed by a similar catalytic cycle to that of binaphos. On the basis of Herrmann's model and CAChe MM2 calculations, we extrapolate that there are two possible transition states (**TS I** and **TS II**, as shown in Figure 1) in the processing of styrene (labeled as green), which represents a typical olefin substrate herein, insertion into the Rh–H bond of [RhH(CO){(*R,S*)-**9b**}]. Both approaches of styrene to the Rh center afford the same configuration (*R*)-2-phenylpropanal. From the stick models for **TS I** and **TS II** based on the

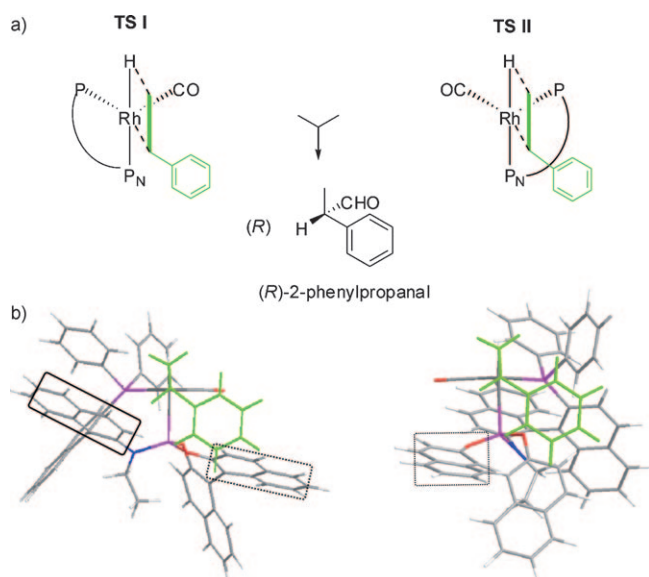


Figure 1. a) Models for two possible transition states, **TS I** and **TS II**, for styrene insertion into the Rh–H bond of  $[\text{RhH}(\text{CO})\{(\text{R},\text{S})\text{-9b}\}]$ . b) Stick models for the corresponding transition states **TS I** and **TS II** based on CAChe MM2 calculations (black rectangle represents naphthyl fragments from the backbone, dashed rectangles represent naphthyl from the phosphoramidite moiety).

results of CAChe MM2 calculations, it is concluded that the enantioselectivity arises from the steric repulsion between the phenyl group of styrene and one of the naphthyl fragments of  $(\text{R},\text{S})\text{-9b}$  (marked with black rectangle in Figure 1).<sup>[17]</sup> In **TS I**, it is the naphthyl from naphthylamine, while it is the one from phosphoramidite in **TS II**. This model can rationalize our experiment results well. As shown in Figure 1, the ethyl group on the N atom stretches back away from the plane of the Rh–H bond and does not interact with the styrene at all. Thus changing the N-substituent did not exert a significant influence on the enantioselectivity of the phosphine–phosphoramidite ligands (Table 2, entries 1–3). Increasing the steric bulkiness of the phosphoramidite fragment (marked as a dashed rectangle in Figure 1) will increase the repulsion to the phenyl ring of styrene and diminish the energy gap between the *Re* and *Si* binding of styrene to the Rh center in **TS I**, although it is somewhat beneficial to the differentiation of two enantiofaces in **TS II**. The overall effect will damage the enantioselectivity of our ligands. Hereby,  $(\text{R},\text{S})\text{-9d}$  provided lower enantioselectivity for all the three substrates than  $(\text{R},\text{S})\text{-9b}$ . Similarly,  $(\text{R},\text{S})\text{-9e}$ , with two bulky *tert*-butyl groups on the phosphoramidite fragment, has even worse enantioselectivity (Table 2, entries 4–6).

It is hard to predict the regioselectivities of the phosphine–phosphoramidite ligands with this theoretical model. Generally, the regioselectivity of the hydroformylation reaction is mainly determined by the functional group on the olefin, for example, the phenyl group in styrene.<sup>[18]</sup> The higher chelation stability with the Rh center the functional group has, the more branched aldehyde will form. In our ex-

periment, for styrene, a trend was observed that the ligand with more bulky substituent provides better regioselectivity.

Encouraged by the successful application of ligand **9b** in the Rh-catalyzed AHF of styrene and vinyl acetate, a series of their derivatives was hydroformylated by utilizing the Rh- $(\text{R},\text{S})\text{-9b}$  catalyst under the optimized reaction conditions. All the styrene derivatives displayed good regioselectivities and excellent enantioselectivities (up to 99% *ee*, Table 3, entries 1–6). The halogen-substituted styrene deriv-

Table 3. Rh-catalyzed AHF of styrene and vinyl acetate derivatives with  $(\text{R},\text{S})\text{-9b}$ .<sup>[a]</sup>

$$\text{R}-\text{CH}=\text{CH}_2 \xrightarrow[\text{CO}/\text{H}_2, \text{Benzene}]{[\text{Rh}(\text{acac})(\text{CO})_2]/(\text{R},\text{S})\text{-9b}} \text{R}-\text{CH}_2-\text{CHO} + \text{R}-\text{CH}(\text{R})-\text{CHO}$$

Entry	R	Conv. [%] <sup>[b]</sup>	b/l <sup>[b]</sup>	<i>ee</i> [%] <sup>[c]</sup>
1	<i>p</i> -Me-Ph	98	7	99( <i>R</i> )
2	<i>p</i> -F-Ph	99	7	98( <i>R</i> )
3	<i>o</i> -F-Ph	99	10	98( <i>R</i> )
4	<i>p</i> -Cl-Ph	99	7	98( <i>R</i> )
5	<i>p</i> -MeO-Ph	97	6	98( <i>R</i> )
6	<i>p</i> - <i>i</i> Bu-Ph	98	8	98( <i>R</i> )
7	CH <sub>3</sub> CH <sub>2</sub> COO	67	24	93( <i>S</i> )
8	CH <sub>3</sub> (CH <sub>2</sub> ) <sub>2</sub> COO	53	16	94( <i>S</i> )
9	CH <sub>3</sub> (CH <sub>2</sub> ) <sub>6</sub> COO	56	16	94( <i>S</i> )
10	CH <sub>3</sub> (CH <sub>2</sub> ) <sub>8</sub> COO	69	16	96( <i>S</i> )
11	<i>t</i> BuCOO	40	16	98( <i>S</i> )
12	PhCOO	69	24	93( <i>S</i> )

[a] All reactions were carried out at 60 °C in benzene with L:Rh=4:1, substrate/catalyst=1000, 20 bar 1:1 CO/H<sub>2</sub>, and 24 h. [b] Conversions, branched/linear ratio were determined based on <sup>1</sup>H NMR spectroscopy. [c] Determined by GC analysis. The absolute configuration was assigned by comparing the sign of the optical rotations with those in the literature.<sup>[14]</sup>

atives in particular achieved high *ee* values at high conversion (Table 3, entries 2–4). Notably, 98% *ee* was achieved for the *para*-isobutyl styrene (Table 3, entry 6). Its aldehyde product could be oxidized into ibuprofen, one of the most widely used nonsteroidal anti-inflammatory drugs. As shown in Table 3, entries 7–12, a series of vinyl acetate derivatives was hydroformylated with this catalyst system. Remarkably, the AHF of a 2,2-dimethylpropionic acid vinyl ester, bearing a bulky alkyl residue on the carboxyl group, demonstrates the highest enantioselectivity (98% *ee*, Table 2, entry 6). In general, all of the styrene and vinyl acetate derivatives achieved high regio- and enantioselectivities in the Rh-**9b**-catalyzed AHF, which makes this methodology potentially interesting to industrial application.

## Conclusions

In summary, a series of hybrid phosphine–phosphoramidite ligands has been developed and systematically applied in the Rh-catalyzed AHF of styrene, vinyl acetate, allyl cyanide, and their derivatives with high regio- and enantioselectivities under mild conditions. With ligand **9b**, 99% *ee* for styrene derivatives, 98% *ee* for vinyl acetate derivatives, and

96% *ee* for allyl cyanide were achieved, which represents the best results to date. The relationship between the substituent and the enantioselectivity of the ligands was deduced, which was successfully rationalized by Herrmann's theoretical model by CAChe MM2 calculations. Further studies aimed at a better understanding of the origin of the selectivity of phosphine–phosphoramidite ligands and their application in other metal-catalyzed transformations are in progress and will be reported in due course.

## Experimental Section

**General methods:** All reactions and manipulations that were sensitive to moisture or air were performed in a nitrogen-filled glovebox or using standard Schlenk techniques, unless otherwise noted. Solvents were dried with standard procedures and degassed with N<sub>2</sub>. Column chromatography was performed by using 200–400 mesh silica gel supplied by Natland International Corp. Thin-layer chromatography (TLC) was performed on EM reagents 0.25 mm silica 60-F plates. <sup>1</sup>H, <sup>13</sup>C, and <sup>31</sup>P NMR spectra were recorded in CDCl<sub>3</sub> or CD<sub>2</sub>Cl<sub>2</sub> on a Bruker Avance 400 MHz spectrometer or a Varian Mercury 500 MHz FT-NMR spectrometer. Optical rotation was obtained on a Perkin–Elmer 341 MC polarimeter. HRMS were recorded on a Thermo LTQ Orbitrap hybrid mass spectrometer. GC analysis was carried out on Hewlett–Packard 7890 gas chromatograph using chiral capillary columns. Compounds (*S*)-**7a**–(*S*)-**7c**,<sup>[12]</sup> (*R*)-**7b**,<sup>[10]</sup> **8a**,<sup>[9b]</sup> **8d**,<sup>[9d]</sup> **8e**,<sup>[18]</sup> and **8f**<sup>[18]</sup> were synthesized according to the corresponding literature procedures.

**A typical procedure for the preparation of ligand 9:** The synthesis of **9b** was reported in previous work.<sup>[10]</sup> Ligands **9a**, **9c**, and **9d** were prepared following a similar procedure. A typical procedure for (*S,R*)-**9a** is as follows: *n*BuLi (1.2 mmol, 0.48 mL of 2.5 M hexane solution) was added dropwise to a solution of (*S*)-**7a** (480 mg, 1.0 mmol) in anhydrous THF (10 mL) at –78 °C under an N<sub>2</sub> atmosphere. The reaction mixture turned deep red and was stirred for 4 h at that temperature. Then (*R*)-**8a** (454 mg, 1.3 mmol) in THF (6 mL) was added dropwise. After addition, the reaction mixture was allowed to warm to room temperature and stirred overnight. The volatiles were removed under vacuum. CH<sub>2</sub>Cl<sub>2</sub> (5 mL) was added to the residue, and the mixture was filtered to remove the inorganic salt. The filtrate was concentrated and subjected to flash chromatography on silica gel (eluted with hexane/EtOAc/NEt<sub>3</sub> 100:10:1) to afford pure ligand (*S,R*)-**9a** (257 mg) as a white solid in 33% yield. [ $\alpha$ ]<sub>D</sub><sup>20</sup> = –32.6 (*c* = 0.3, CHCl<sub>3</sub>); <sup>1</sup>H NMR (500 MHz, CDCl<sub>3</sub>):  $\delta$  = 8.04–8.01 (m, 3H), 7.85 (t, *J* = 8.5 Hz, 2H), 7.78 (d, *J* = 8.5 Hz, 2H), 7.68 (d, *J* = 9.0 Hz, 1H), 7.61–7.57 (m, 2H), 7.38–6.93 (m, 21H), 6.59 (dd, *J* = 8.5, 7.0 Hz, 1H), 6.49 (d, *J* = 8.5 Hz, 1H), 6.31 (d, *J* = 8.5 Hz, 1H), 2.45 ppm (s, 3H); <sup>13</sup>C NMR (125 MHz, CDCl<sub>3</sub>):  $\delta$  = 150.45, 150.41, 149.61, 142.76, 142.49, 138.60, 138.49, 137.88, 137.79, 136.63, 135.25, 135.07, 134.08, 133.16, 133.03, 132.65, 131.61, 131.50, 130.73, 130.28, 129.94, 129.87, 128.84, 128.48, 128.31, 128.28, 128.20, 128.02, 127.75, 127.56, 127.42, 127.24, 127.16, 126.99, 126.53, 126.09, 125.69, 125.35, 124.86, 124.64, 124.12, 124.08, 122.28, 122.20, 35.67, 35.64 ppm; <sup>31</sup>P NMR (202 MHz, CDCl<sub>3</sub>):  $\delta$  = 141.09 (d, *J* = 45.2 Hz), –12.67 ppm (d, *J* = 45.2 Hz); HRMS (ESI): *m/z*: calcd for C<sub>53</sub>H<sub>38</sub>NO<sub>2</sub>P<sub>2</sub> ([*M*+H]<sup>+</sup>): 782.2578; found: 782.2374. Ligands **9b–f** were synthesized in moderate yields following the above procedure. Their characterization data are summarized as follows.

**(*S,R*)-9b:** Yield = 38%; white solid; [ $\alpha$ ]<sub>D</sub><sup>20</sup> = –18.3 (*c* = 0.4, CHCl<sub>3</sub>); <sup>1</sup>H NMR (400 MHz, CDCl<sub>3</sub>):  $\delta$  = 8.07–7.98 (m, 3H), 7.90 (t, *J* = 7.3 Hz, 2H), 7.78 (d, *J* = 8.2 Hz, 2H), 7.64–7.57 (m, 4H), 7.38–6.99 (m, 16H), 6.96 (t, *J* = 6.8 Hz, 2H), 6.85 (t, *J* = 7.1 Hz, 2H), 6.55 (t, *J* = 7.7 Hz, 1H), 6.38–6.29 (m, 2H), 2.75–2.67 (m, 1H), 2.37–2.29 (m, 1H), 0.65 ppm (t, *J* = 7.0 Hz, 3H); <sup>13</sup>C NMR (100 MHz, CDCl<sub>3</sub>):  $\delta$  = 150.29, 150.22, 149.94, 142.34, 141.95, 138.57, 138.36, 138.27, 138.20, 135.44, 135.14, 134.10, 133.57, 133.36, 131.68, 130.50, 129.88, 129.11, 128.66, 128.59, 128.55, 128.49, 128.46, 128.42, 128.30, 128.12, 127.56, 127.19, 127.12, 127.03, 126.66, 126.29, 126.17, 125.71, 125.53, 125.06, 124.76, 122.49, 122.24,

122.21, 41.05, 14.99 ppm; <sup>31</sup>P NMR (162 MHz, CDCl<sub>3</sub>):  $\delta$  = 141.00 (d, *J* = 59.1 Hz), –13.48 ppm (d, *J* = 59.1 Hz); HRMS (ESI): *m/z*: calcd for C<sub>54</sub>H<sub>40</sub>NO<sub>2</sub>P<sub>2</sub> ([*M*+H]<sup>+</sup>): 796.2534; found: 796.2536.

**(*S,R*)-9c:** Yield = 42%; white solid; [ $\alpha$ ]<sub>D</sub><sup>20</sup> = +32.5 (*c* = 0.3, CHCl<sub>3</sub>); <sup>1</sup>H NMR (500 MHz, CDCl<sub>3</sub>):  $\delta$  = 8.17 (d, *J* = 8.5 Hz, 1H), 8.15 (d, *J* = 8.0 Hz, 1H), 7.97 (d, *J* = 8.0 Hz, 1H), 7.92 (d, *J* = 8.0 Hz, 1H), 7.74–7.60 (m, 5H), 7.43–7.01 (m, 23H), 6.87–6.83 (m, 2H), 6.79–6.75 (m, 2H), 6.45–6.42 (m, 1H), 6.24 (d, *J* = 8.5 Hz, 1H), 5.93 (d, *J* = 8.5 Hz, 1H), 3.82 (d, *J* = 14.5 Hz, 1H), 3.21 (d, *J* = 14.5 Hz, 1H); <sup>13</sup>C NMR (125 MHz, CDCl<sub>3</sub>):  $\delta$  = 150.09, 150.05, 149.84, 142.04, 141.91, 138.75, 128.24, 127.92, 137.81, 135.61, 135.42, 133.97, 133.56, 133.43, 132.01, 131.81, 131.75, 131.61, 130.72, 130.50, 130.35, 129.87, 129.81, 128.83, 128.74, 128.56, 128.48, 128.40, 128.37, 128.33, 128.21, 128.11, 128.04, 127.89, 127.84, 127.79, 127.40, 127.23, 127.20, 127.04, 126.88, 126.71, 126.08, 126.03, 125.32, 124.88, 124.63, 122.78, 122.55, 122.10, 51.32 ppm; <sup>31</sup>P NMR (202 MHz, CDCl<sub>3</sub>):  $\delta$  = 138.41 (d, *J* = 78.6 Hz), –11.86 ppm (d, *J* = 78.6 Hz); HRMS (ESI): *m/z*: calcd for C<sub>59</sub>H<sub>42</sub>NO<sub>2</sub>P<sub>2</sub> ([*M*+H]<sup>+</sup>): 858.2691; found: 858.2692.

**(*R,S*)-9d:** Yield = 41%; white solid; [ $\alpha$ ]<sub>D</sub><sup>20</sup> = –15.9 (*c* = 0.1, CHCl<sub>3</sub>); <sup>1</sup>H NMR (400 MHz, CD<sub>2</sub>Cl<sub>2</sub>):  $\delta$  = 8.04–7.96 (m, 3H), 7.86–7.79 (m, 3H), 7.72 (d, *J* = 8.0 Hz, 1H), 7.68 (d, *J* = 8.4 Hz, 1H), 7.53–7.45 (m, 2H), 7.39–7.28 (m, 5H), 7.26–7.05 (m, 11H), 6.96–6.93 (m, 2H), 6.86–6.81 (m, 2H), 6.61–6.57 (m, 1H), 6.33 (d, *J* = 8.4 Hz, 1H), 2.94–2.83 (m, 1H), 2.58 (s, 3H), 2.50–2.45 (m, 1H), 1.66 (s, 3H), 0.70 ppm (t, *J* = 7.2 Hz, 3H); <sup>13</sup>C NMR (100 MHz, CD<sub>2</sub>Cl<sub>2</sub>):  $\delta$  = 150.19, 150.12, 149.84, 142.23, 141.90, 138.93, 138.61, 138.57, 138.34, 137.72, 135.86, 135.34, 135.12, 134.41, 134.11, 133.94, 133.75, 133.74, 132.18, 132.01, 131.75, 131.68, 131.23, 131.07, 130.80, 130.06, 129.49, 129.09, 128.91, 128.58, 128.48, 128.29, 128.21, 127.93, 127.64, 127.29, 127.11, 127.02, 126.66, 125.80, 125.56, 125.32, 125.23, 125.07, 124.73, 121.81, 41.54, 17.66, 14.76 ppm; <sup>31</sup>P NMR (162 MHz, CD<sub>2</sub>Cl<sub>2</sub>):  $\delta$  = 139.00 (d, *J* = 61.6 Hz), –14.60 ppm (d, *J* = 61.6 Hz); HRMS (ESI): *m/z*: calcd for C<sub>56</sub>H<sub>44</sub>NO<sub>2</sub>P<sub>2</sub> ([*M*+H]<sup>+</sup>): 824.2847; found: 824.2843.

**(*R,S*)-9e:** Yield = 38%; white solid; [ $\alpha$ ]<sub>D</sub><sup>20</sup> = +91.7 (*c* = 0.5, CHCl<sub>3</sub>); <sup>1</sup>H NMR (400 MHz, CDCl<sub>3</sub>):  $\delta$  = 7.98 (d, *J* = 8.8 Hz, 1H), 7.93 (d, *J* = 8.4 Hz, 1H), 7.89 (d, *J* = 8.4 Hz, 1H), 7.83 (d, *J* = 8.0 Hz, 1H), 7.72 (d, *J* = 8.8 Hz, 1H), 7.63 (dd, *J* = 8.4, 2.4 Hz, 1H), 7.50–7.46 (m, 1H), 7.24–7.12 (m, 6H), 7.06–6.87 (m, 9H), 6.65 (t, *J* = 8.0 Hz, 1H), 3.58–3.50 (m, 1H), 2.80–2.73 (m, 1H), 2.23 (s, 3H), 2.20 (s, 3H), 1.78 (s, 3H), 1.76 (s, 3H), 1.34 (s, 9H), 0.81 (t, *J* = 7.2 Hz, 3H), 0.74 ppm (s, 9H); <sup>13</sup>C NMR (100 MHz, CDCl<sub>3</sub>):  $\delta$  = 148.95, 148.84, 147.74, 147.69, 142.72, 142.39, 138.85, 138.69, 138.46, 137.80, 137.77, 136.43, 135.12, 134.89, 134.57, 134.31, 134.05, 133.68, 133.29, 133.23, 133.13, 133.07, 131.80, 131.73, 131.25, 131.05, 130.76, 129.55, 129.38, 128.13, 128.06, 128.03, 127.72, 127.64, 127.46, 127.25, 127.20, 126.64, 126.55, 125.75, 125.15, 124.70, 40.05, 34.63, 34.07, 31.29, 31.26, 30.05, 20.19, 16.80, 16.31, 13.06 ppm; <sup>31</sup>P NMR (162 MHz, CDCl<sub>3</sub>):  $\delta$  = 130.50 (d, *J* = 97.2 Hz), –14.89 ppm (d, *J* = 97.2 Hz); HRMS (ESI): *m/z*: calcd for C<sub>58</sub>H<sub>60</sub>NO<sub>2</sub>P<sub>2</sub> ([*M*+H]<sup>+</sup>): 864.4099; found: 864.4105.

**(*R*)-9f:** Yield = 52%; white solid; [ $\alpha$ ]<sub>D</sub><sup>20</sup> = +40.7 (*c* = 0.5, CHCl<sub>3</sub>); <sup>1</sup>H NMR (400 MHz, CDCl<sub>3</sub>):  $\delta$  = 7.91 (d, *J* = 7.2 Hz, 1H), 7.83 (d, *J* = 8.4 Hz, 2H), 7.73 (d, *J* = 8.4 Hz, 2H), 7.50 (dd, *J* = 7.2, 2.8 Hz, 1H), 7.39 (t, *J* = 7.2 Hz, 1H) 7.24–7.00 (m, 11H), 6.97–6.93 (m, 4H), 6.85 (t, *J* = 7.6 Hz, 2H), 6.51–6.47 (m, 1H), 6.27 (d, *J* = 8.4 Hz, 1H), 3.39–3.32 (m, 1H), 3.06–2.97 (m, 1H), 1.24 (s, 9H), 1.23 (s, 9H), 1.04–0.98 (m, 18H), 0.82 ppm (t, *J* = 6.4 Hz, 3H); <sup>13</sup>C NMR (100 MHz, CDCl<sub>3</sub>):  $\delta$  = 147.50, 147.40, 146.82, 146.77, 144.32, 144.26, 143.68, 143.63, 138.82, 138.49, 137.93, 137.77, 136.99, 136.85, 133.97, 133.74, 133.48, 133.42, 133.12, 132.29, 132.22, 132.02, 131.97, 131.85, 131.80, 131.48, 130.24, 129.84, 129.73, 128.01, 127.79, 127.24, 127.05, 126.96, 126.87, 126.79, 126.68, 126.63, 126.39, 126.19, 126.14, 125.95, 125.77, 125.40, 125.04, 124.28, 124.14, 123.98, 122.77, 122.74, 37.77, 34.09, 33.67, 33.53, 33.45, 30.53, 30.49, 29.73, 29.34, 20.43 ppm; <sup>31</sup>P NMR (162 MHz, CDCl<sub>3</sub>):  $\delta$  = 136.29 (br), –14.93 ppm (d, *J* = 62.4 Hz); HRMS (ESI): *m/z*: calcd for C<sub>62</sub>H<sub>68</sub>NO<sub>2</sub>P<sub>2</sub> ([*M*+H]<sup>+</sup>): 920.4725; found: 920.4749.

**General procedure for asymmetric hydroformylation:** In a glovebox filled with nitrogen, to a 2 mL vial equipped with a magnetic bar was added ligand **9** (0.004 mmol), [Rh(acac)(CO)<sub>2</sub>] (0.001 mmol in 0.10 mL

solvent), dodecane (50  $\mu\text{L}$ , as a GC internal standard, if applicable), and substrate (1.0 mmol), additional solvent was charged to bring the total volume of the reaction mixture to 1.0 mL. After the mixture had been stirred for 10 min, the vial was transferred into an autoclave and taken out of the glovebox. Carbon monoxide (10 atm) and dihydrogen (10 atm) were charged in sequence. The reaction mixture was stirred at 60 °C (oil bath) for 24 h. The reaction mixture was cooled and the pressure was carefully released in a well-ventilated hood. For analysis of the products of styrene and vinyl acetate, the conversion, regioselectivity, and enantiomeric excesses were determined following the reported method with a Supelco's Beta Dex 225 column.<sup>[5b]</sup> For analysis of the products of allyl cyanide, the conversion and regioselectivity were determined by GC with a Supelco's Beta Dex 120 column.<sup>[6]</sup> The enantiomeric excesses of product **17** were determined by oxidation with Jones reagent to afford the corresponding carboxylic acid, followed by reaction with aniline to give the corresponding amide, which was analyzed by HPLC (Column: Chiralcel AS; solvent: hexane/*i*PrOH=80:20; flow: 1.0 mL min<sup>-1</sup>; 254 nm; (S) enantiomer:  $t_{\text{R}}=7.75$  min, (R) enantiomer:  $t_{\text{R}}=9.74$  min). For styrene and vinyl acetate derivatives, the conversion and regioselectivity were determined by <sup>1</sup>H NMR spectroscopy from the crude reaction mixture. The enantiomeric excesses of the hydroformylation products were determined by GC with Supelco's Beta Dex 225 column (for details see Supporting Information).

### Acknowledgements

We thank the National Institutes of Health (GM58832) and Merck & Co., Inc. for financial support. The Bruker 400 MHz NMR spectrometer used in these studies was purchased with grant No. 1S10RR023698-01A1 from the National Center for Research Resources (NCRR), a component of NIH.

- [1] For reviews, see: a) C. Claver, P. W. N. M. van Leeuwen in *Rhodium Catalyzed Hydroformylation*, Vol. 22 (Eds.: C. Claver, P. W. N. M. van Leeuwen), Kluwer Academic Publishers, Dordrecht, **2000**; b) F. Agbossou, J. F. Carpentier, A. Mortreux, *Chem. Rev.* **1995**, *95*, 2485–2506; c) W. A. Herrmann, B. Cornils, *Angew. Chem.* **1997**, *109*, 1074–1095; *Angew. Chem. Int. Ed. Engl.* **1997**, *36*, 1048–1067; d) K. Nozaki, I. Ojima in *Catalytic Asymmetric Synthesis*, 2nd ed. (Ed.: I. Ojima), Wiley-VCH, Weinheim, **2000**, Chapter 7; e) B. Breit, W. Seiche, *Synthesis* **2001**, 1–36; f) B. Breit, *Angew. Chem.* **2005**, *117*, 6976–6986; *Angew. Chem. Int. Ed.* **2005**, *44*, 6816–6825.
- [2] For recent reviews on AHF, see: a) M. Diéguez, O. Pàmies, C. Claver, *Tetrahedron: Asymmetry* **2004**, *15*, 2113–2122; b) C. Claver, M. Dieguez, O. Pamies, S. Castillon, *Top. Organomet. Chem.* **2006**, *18*, 35–64; c) J. Klosin, C. R. Landis, *Acc. Chem. Res.* **2007**, *40*, 1251–1259.
- [3] a) J. K. Still in *Comprehensive Organic Synthesis*, Vol. 4 (Eds.: B. M. Trost, I. Fleming, L. A. Paquette), Pergamon Press, Oxford, **1991**, pp. 913–950; b) T. Šmejkal, B. Breit, *Angew. Chem.* **2008**, *120*, 317–321; *Angew. Chem. Int. Ed.* **2008**, *47*, 311–315.
- [4] a) J. E. Babin, G. T. Whiteker (Union Carbide Corporation), WO 9303839, **1993**; b) G. T. Whiteker, J. R. Briggs, J. E. Babin, B. A. Barner, *Chemical Industries*, Vol. 89, Marcel Dekker, New York, **2003**, pp. 359–367.
- [5] a) C. J. Copley, K. Gardner, J. Klosin, C. Praquin, C. Hill, G. T. Whiteker, A. Zanotti-Gerosa, J. L. Petersen, K. A. Abboud, *J. Org. Chem.* **2004**, *69*, 4031–4040; b) C. J. Copley, J. Klosin, C. Qin, G. T. Whiteker, *Org. Lett.* **2004**, *6*, 3277–3280.
- [6] S. Breeden, D. J. Cole-Hamilton, D. F. Foster, G. J. Schwarz, M. Wills, *Angew. Chem.* **2000**, *112*, 4272–4274; *Angew. Chem. Int. Ed.* **2000**, *39*, 4106–4108.
- [7] a) T. P. Clark, C. R. Landis, S. L. Freed, J. Klosin, K. Abboud, *J. Am. Chem. Soc.* **2005**, *127*, 5040–5042; b) A. T. Axtell, C. J. Copley, J. Klosin, G. T. Whiteker, A. Zanotti-Gerosa, K. A. Abboud, *Angew. Chem.* **2005**, *117*, 5984–5988; *Angew. Chem. Int. Ed.* **2005**, *44*, 5834–5838; c) P. J. Thomas, A. T. Axtell, J. Klosin, W. Peng, C. L. Rand, T. P. Clark, C. R. Landis, K. A. Abboud, *Org. Lett.* **2007**, *9*, 2665–2668.
- [8] B. Zhao, X. Peng, Z. Wang, C. Xia, K. Ding, *Chem. Eur. J.* **2008**, *14*, 7847–7857.
- [9] a) N. Sakai, S. Mano, K. Nozaki, H. Takaya, *J. Am. Chem. Soc.* **1993**, *115*, 7033–7034; b) K. Nozaki, N. Sakai, T. Nanno, T. Higashijima, S. Mano, T. Horiuchi, H. Takaya, *J. Am. Chem. Soc.* **1997**, *119*, 4413–4423; c) T. Horiuchi, T. Ohta, E. Shirakawa, K. Nozaki, H. Takaya, *J. Org. Chem.* **1997**, *62*, 4285–4292; d) T. Horiuchi, E. Shirakawa, K. Nozaki, H. Takaya, *Organometallics* **1997**, *16*, 2981–2986; e) K. Nozaki, T. Matsuo, F. Shibahara, T. Hiyama, *Adv. Synth. Catal.* **2001**, *343*, 61–63; f) F. Shibahara, K. Nozaki, T. Hiyama, *J. Am. Chem. Soc.* **2003**, *125*, 8555–8560.
- [10] Y. Yan, X. Zhang, *J. Am. Chem. Soc.* **2006**, *128*, 7198–7202.
- [11] For figures of the space-filling and stick models (based on CAChe MM2 calculations) see reference [10].
- [12] a) K. Sumi, T. Ikariya, R. Noyori, *Can. J. Chem.* **2000**, *78*, 697–703; b) T. Morimoto, N. Mochizuki, M. Suzuki, *Tetrahedron Lett.* **2004**, *45*, 5717–5722.
- [13] S. Vyskocil, M. Smrcina, V. Hanus, M. Polasek, P. Kocovsky, *J. Org. Chem.* **1998**, *63*, 7738–7748.
- [14] a) G. Consiglio, P. Pino, L. I. Flowers Jr., C. U. Pittman, *J. Chem. Soc. Chem. Commun.* **1983**, 612–613; b) S. G. Cohen, J. Crossley, E. Khedouri, R. Zand, L. H. Klee, *J. Am. Chem. Soc.* **1963**, *85*, 1685–1691; lit c) Z.-F. Xie, H. Suemune, K. Sakai, *Tetrahedron: Asymmetry* **1993**, *4*, 973–980.
- [15] A. T. Axtell, J. Klosin, K. A. Abboud, *Organometallics* **2006**, *25*, 5003–5009.
- [16] D. Gleich, R. Schmid, W. A. Herrmann, *Organometallics* **1998**, *17*, 2141–2143.
- [17] This theoretical model does not take account of the chelation of the olefin functionality with the Rh center, which can also influence the enantioface selection during or prior to the insertion step somewhat. Meanwhile, we cannot rule out the possibility that both the steps of Rh-alkyl and Rh-acyl formation are reversible. In such a situation, the enantioselectivity will be affected in the final product-forming Rh-acyl hydrogenolysis step.
- [18] C. J. Copley, R. D. J. Froese, J. Klosin, C. Qin, G. T. Whiteker, K. A. Abboud, *Organometallics* **2007**, *26*, 2986–2999.

Received: August 11, 2009  
Published online: November 30, 2009